JOURNAL OF APPLIED ELECTROCHEMISTRY 11 (1981) 543–549

Morphological characteristics of copper deposition on stainless steel cathodes

M. I. ISMAIL, T. Z. FAHIDY

Department of Chemical Engineering, University of Waterloo, Waterloo, Ontario, Canada N2L 3G1

Received 10 September 1980

The results of a metallographic study of cathodic copper deposition on 316 stainless steel are presented. In magnetically assisted d.c. electrolysis, characteristic screen-type deposition patterns are observed. Simultaneous hydrogen evolution causes tunnel-type deposits at 30–45° to the horizontal.

Nomenclature

B_z	magnetic flux density, vertical field lines pointing downwards
C	electrolyte concentration
CVD	cell voltage drop
i_c	cathode current density
s	cathode–anode separation distance
T	temperature
t_e	length of electrolysis time

1. Introduction

In numerous industrial and research applications, especially in catalysis, the effectiveness of the metal surface is strongly linked to the high state of dispersion of the metal on the substrate surface. One interesting form of dispersion is the fine-mesh (less than 1 mm opening size) metal screen which is deposited electrolytically on a substrate metal cathode and which adheres to the substrate but can easily be removed by careful peeling. As shown in previous publications [1, 2], copper screens can be deposited on type 316 stainless steel cathodes while electrolysing aqueous cupric sulphate solutions. Here simultaneous hydronium-ion discharge and subsequent hydrogen gas evolution on the cathode surface are primarily responsible for the particular screen structure, whose characteristics are strongly influenced by imposed magnetic fields. Preliminary information on this effect, obtained in a pilot-plant-scale apparatus, indicated that the influence of the magnetic field on the process could not be interpreted in simple terms and that a deeper investigation of fundamental phenomena in a laboratory-scale cell was warranted. This paper presents the summary of a study where the effect of *uniform* magnetic fields on the morphological properties of the screen-type deposit was investigated. It is expected that the results will contribute to the currently incomplete understanding of the magnetic field effect and to a more efficient design of (magnetoelectrolytic) metal deposition processes.

2. Apparatus and results

The experimental cell, a small-scale facsimile of the pilot-size reactor previously studied [1, 2], consisted of type 316 stainless steel pieces of size 60 mm x 10 mm x 0.8 mm placed in a 35 mm i.d., 55 mm high cylindrical Pyrex cell, at a separation of 8 mm. Before each experiment the electrodes were degreased and polished mechanically using emery papers up to grade 600. The electrolyte was a 0.6 mol dm^{-3} aqueous $CuSO_4$ solution with a pH variation between 3.56 (15° C) and 3.11 (85° C) in the experimental temperature range. Electrolysis was carried out by means of a conventional regulated power supply at preset values of potential drop or current flow between the pole faces of a 5 kW Walker Model 7 d.c. electromagnet energized by a regulated power supply of 0.0002–0.001% stability [3]. During electrolysis the strength of the magnetic field was held at a predetermined value. The cathodes were carefully dried after electrolysis and were photographed

0021–891X/81/050543–07$02.70/0

Table 1. The variation of cell current flow with magnetic field strength at selected cell voltage drops and electrode separations. Electrolyte concentration: 1.295 mol dm^{-3} aqueous $CuSO_4$ (25° C); active electrode height: 39 mm; active electrode area: 390 mm^2

Imposed magnetic flux density B_z (mT)	*Cell current flow* (mA)								
	CVD = 1 V			*CVD = 2 V*			*CVD = 3 V*		
	s(mm) = 1.5	8	20	1.5	8	20	1.5	8	20
4 (residual value)	–	2	–	361	212	118	1228	754	320
200	4–7	4	3–9	372	256	118	1303	794	603
324	4–9	3	3–11	444	269	126	1320	817	620
540	7–17	–	3–12	394	241	144	1378	793	607
685	39–24	4	3–18	462	228	124	1320	708	606

under an optical metallurgical microscope at various magnification settings. The magnification range used to examine the prepared surface areas was 50×–800×.

2.1. *Cell behaviour in uniform magnetic fields*

Experiments were carried out between two, approximately 18 cm diameter, pole faces of the regulated d.c. electromagnet. At a pole face separation of approximately 7.6 cm (3 in) the minimal uniformity of the magnetic field was 98.5%. The imposed electric and magnetic fields were transverse in the following configuration: the electric field was horizontal between the vertical electrodes and the magnetic field vertical with the flux density vector pointing downwards. Electrolysis was carried out at predetermined values of the cell voltage drop and magnet-exciting current flow, the latter calibrated for corresponding values of the magnetic flux density. The electrode separation distances and electrolyte concentrations were varied in a preset manner.

Tables 1 and 2 present typical experimental results obtained in this portion of the study. At low voltage drops and very small separation distances the current flow is erratic and fluctuates between approximate limits, as illustrated in Table 1 for a CVD of 1 V (s = 1.5 mm corresponds to one half of the estimated diameter of an O_2 bubble [4]). At higher CVD values and at a high electrolyte concentration (C_0 = 1.295 mol dm^{-3} is very close to the solubility limit of $CuSO_4$) the cell current flow reaches a maximum value which does not usually correspond to the highest magnetic field strength imposed on the cell. However, as the electrolyte concentration is decreased, the current flow tends to increase monotonically with the strength of the magnetic field at a given CVD and separation distance. Taking the value of the current flow observed at the residual magnetic flux density as the nonmagnetic reference value,

Table 2. The variation of cell current flow with magnetic field strength at selected cell voltage drops and electrolyte concentrations. Electrode separation: 8 mm; active electrode height: 39 mm; active electrode area: 390 mm^2; C_0 = 1.295 mol dm^{-3}

Imposed magnetic flux density B_z (mT)	*Cell current flow* (mA)											
	CVD = 2 V				*CVD = 3 V*				*CVD = 3.8 V*	*CVD = 4 V*		
	$C = C_0$	$\frac{1}{4}C_0$	$\frac{1}{8}C_0$	$\frac{1}{32}C_0$	C_0	$\frac{1}{4}C_0$	$\frac{1}{8}C_0$	$\frac{1}{32}C_0$	C_0	$\frac{1}{4}C_0$	$\frac{1}{8}C_0$	$\frac{1}{32}C_0$
4 (residual value)	212	133	61	60	754	403	181	109	1172	635	238	158
200	256	146	85	64	794	471	185	128	1229	810	320	182
374	269	170	105	67	817	473	190	154	1139	850	322	206
540	241	170	121	68	793	575	194	165	1207	870	322	220
685	228	209	124	68	708	500	195	174	1250	793	324	225

relative current increases up to 90% were observed, the usual range being 15–45%, depending on the process variables.

At relatively high concentrations ($0.2C_0 < C \leqslant C_0$) the current flow reaches a maximum at an intermediate value of the magnetic flux density, above which it may drop monotonically or fluctuate when B_0 is further increased. At relatively low concentrations, however, i.e. when $C < \sim 0.2C_0$ the current flow increases with the magnetic flux density and no relative maximum is observed; this phenomenon remains essentially independent of the electrolyte temperature up to about 70° C. Moreover, the ratio of the largest current flow measured in the presence of a magnetic field to the current flow observed at the same electrolyte temperature and cell voltage drop, in the absence of a magnetic field, was found to be virtually independent of the electrolyte temperature within the 30–70° C temperature range (the magnitude of the temperature coefficient is of the order of $-10^{-4}\ °C^{-1}$).

2.2. *Morphological characteristics of the magneto-electrolytic cathode deposits*

Typical deposit patterns observed in the absence of a magnetic field are shown in Fig. 1. An initially copper-free stainless steel surface (Fig. 1a) and copper deposited on the same initially copper-free area (Fig. 1b) are shown side by side; isolated copper deposits (dark areas in Fig. 1c) clearly show grain boundary dissolution at the adjacent stainless steel areas.

Fig. 2 shows a typical deposition growth pattern in a relatively weak magnetic field (B_z = 200 mT) and at short electrolysis times. Crystals at the air–electrolyte interface may grow to a size of about 10 μm in the vertical direction at the beginning of deposition (Fig. 2a); growth is parallel to the magnetic field lines. This process is followed by horizontal crystal growth leading ultimately to screen-type deposition, as depicted by the micrograph of Fig. 2b taken on a surface portion about half-way between the air–electrolyte interface and lower electrode edge. The cathodic screen openings are about 5 μm. The surface of the associated anode is characterized by a somewhat larger (about 7 μm size, uniform grain) microstructure, as shown in Fig. 2c. This screen-type deposition pattern is apparently independent of temperature (at least at practical deposition temperatures) but its propagation parallel to the imposed magnetic field direction has been found to be consistently faster than growth in the horizontal direction, as demonstrated in Fig. 3; the isolated bright areas are partially copper-free substrate 'bands'.

The influence of simultaneous hydrogen evolution at the cathode on the deposition pattern of copper is of considerable interest. In a series of experiments, two specific patterns were observed. The first one, illustrated by Fig. 4, consists of typical local hydrogen evolution sites (Fig. 4a) on the substrate surface, and selective copper deposition (Fig. 4b) around and inside the sites. The second pattern is manifest by local tunnel-like structures appearing at inclination angles of 45° (Fig. 5a) and 30° (Fig. 5b) with respect to the horizontal reference plane. The lamellar structure of the tunnel indicates an alternating copper deposition/H_2 evolution pattern, with parallel H_2 evolution 'lines' in the lamellae. This microstructure is spread out rather evenly over the specimen electrode surface and appears to be independent of position relative to the edges of the electrode.

The morphological characteristics of the anode surface during electrolysis were not examined in detail in this study, but preliminary observations indicate that at locations near the air–electrolyte interface the anode undergoes grain-boundary corrosion and there seems to be selective dissolution parallel to the magnetic field lines. The corrosion channel has an average diameter of about 1.5 μm and the average pit diameter is about 10 μm. Below, but still near, the interface, corrosion is uniform, but selective local dissolution patterns can still be observed parallel to the magnetic field lines.

3. Discussion

The effect of magnetic fields on the current–CVD characteristics cannot be explained at present in a simple manner. One possible interpretation of the experimental observations may be in terms of electrode kinetics: the strength of the magnetic field may affect the kinetics of individual electrode reactions in a specific manner, whereby, within a certain range of flux density, one (or

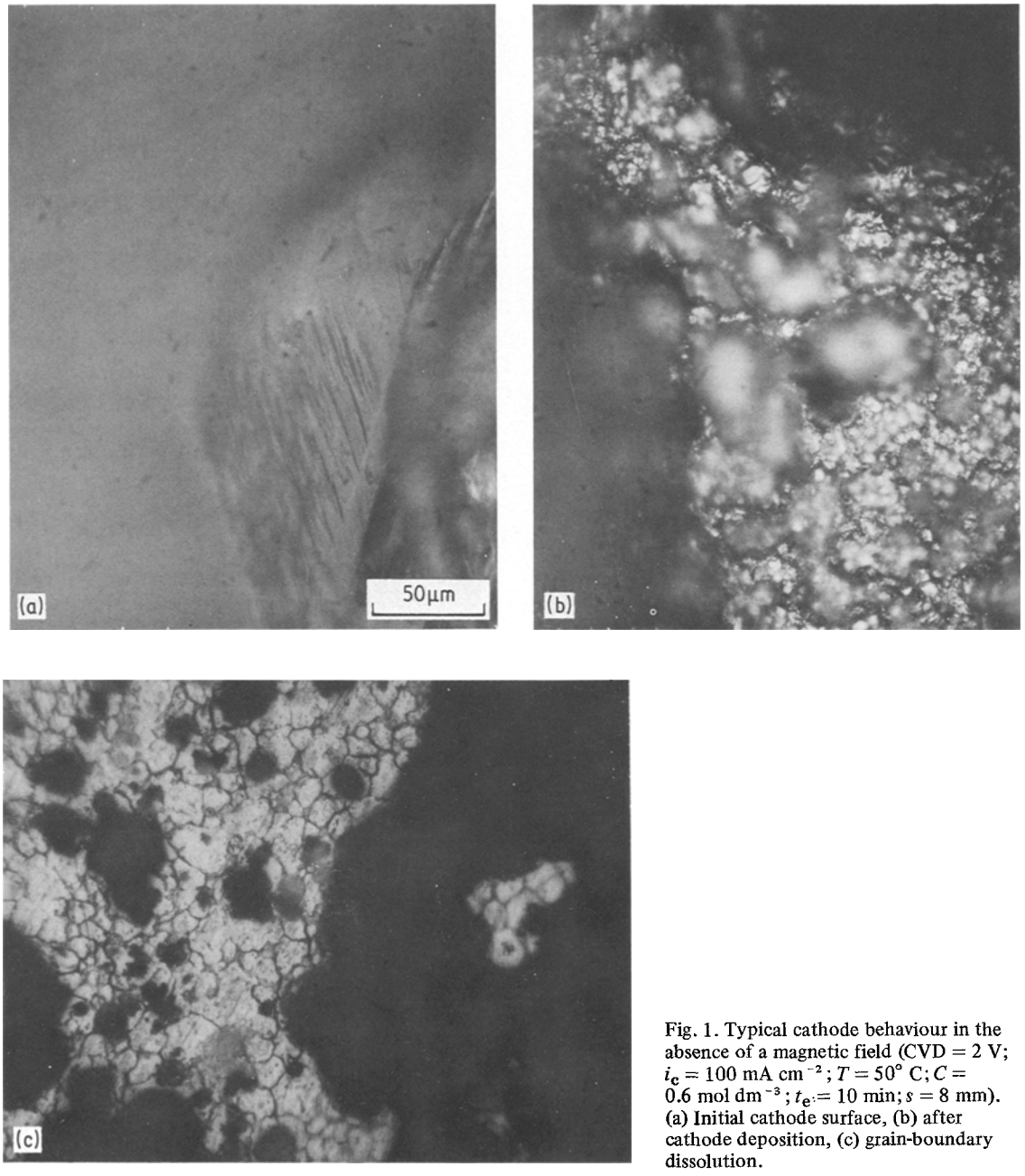

Fig. 1. Typical cathode behaviour in the absence of a magnetic field (CVD = 2 V; $i_c = 100$ mA cm^{-2}; $T = 50°$ C; $C = 0.6$ mol dm^{-3}; $t_e = 10$ min; $s = 8$ mm). (a) Initial cathode surface, (b) after cathode deposition, (c) grain-boundary dissolution.

more) electrode process(es) being predominant, the overall polarization overvoltage increases or decreases. If the CVD is set to a constant value, the resultant current flow is expected to follow inversely this variation in overvoltage. In the light of earlier investigations of the magnetic field effect on polarization phenomena [e.g. 5–9] a reasoning based on relative kinetics appears at least plausible. On the other hand, an interpretation based on magnetohydrodynamic effects brought about by the imposed magnetic field at the electrode surface could presumably be advanced. Further quantitative work will be required before a fully coherent explanation of the magnetic field effect on cathode polarization can be offered.

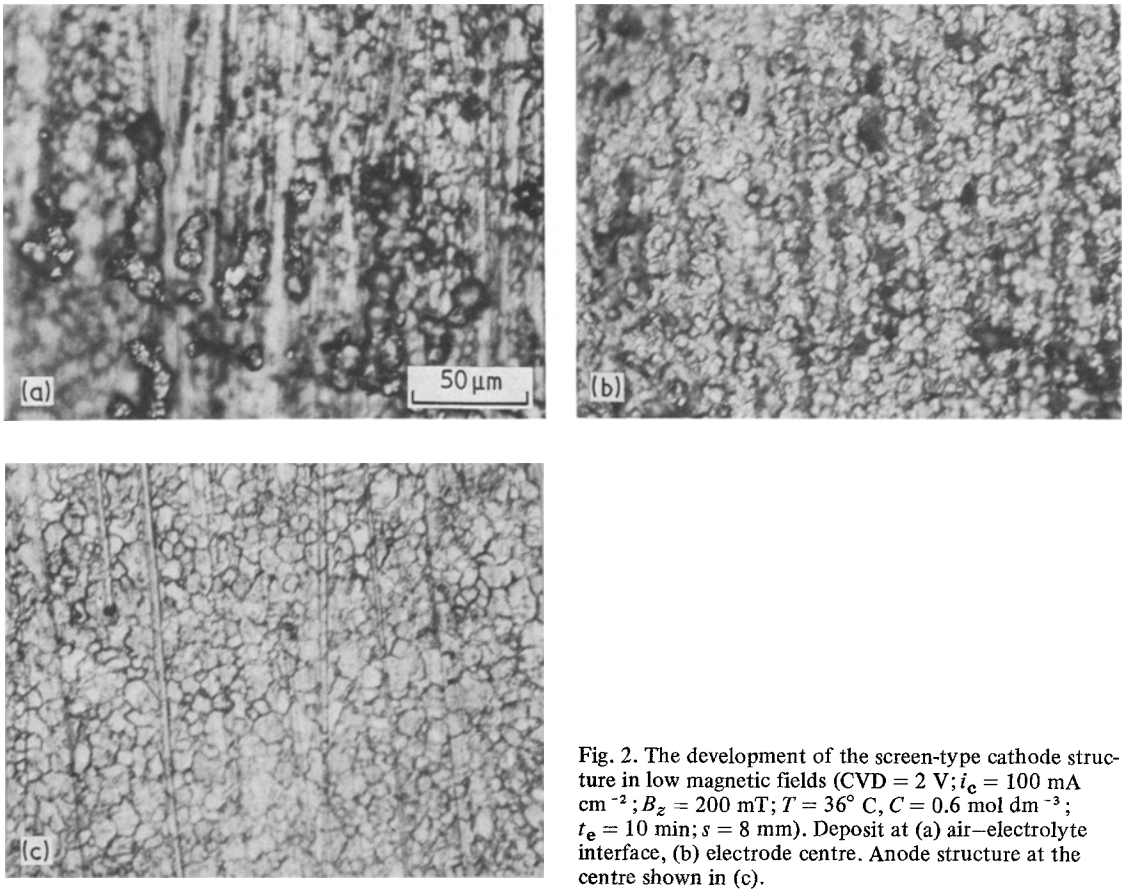

Fig. 2. The development of the screen-type cathode structure in low magnetic fields (CVD = 2 V; i_c = 100 mA cm^{-2}; B_z = 200 mT; T = 36° C, C = 0.6 mol dm^{-3}; t_e = 10 min; s = 8 mm). Deposit at (a) air–electrolyte interface, (b) electrode centre. Anode structure at the centre shown in (c).

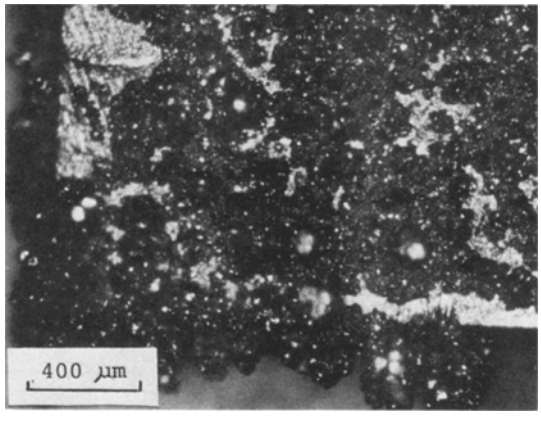

Fig. 3. Typical growth pattern in a uniform magnetic field. The field lines are downwards vertical (CVD = 2.5 V; $i_c \cong$ 150 mA cm^{-2}; B_z = 540 mT; T = 75° C; C = 0.6 mol dm^{-3}; t_e = 7 min; s = 8 mm).

In interpreting the effect of the magnetic field imposition and hydrogen formation on deposit morphology, it is instructive to consider some previous results reported in the associated literature. Twinning is a common feature in face-centered cubic metals and pentagonal structures have also been found in copper electrodeposits [10, 11]. Initial-stage deposition configurations strongly depend on the total bonding energy: if E_s, the bonding energy between metal atom and substrate, is much larger than E_m, the bonding energy between two metal atoms, planar addition of the fourth atom to a three-atom entity will result with a total bonding energy of $5E_m + 4E_s$. If, however, $E_m \gg E_s$, tetrahedral cluster deposition, with a total bonding energy of $6E_m + 3E_s$, will result. The growth of a fresh, closely packed layer on the surface is determined by the position of the first atom pair: if it is in proper lattice sites, perfect crystal growth might ensue. In an imposed magnetic field the migration path at the

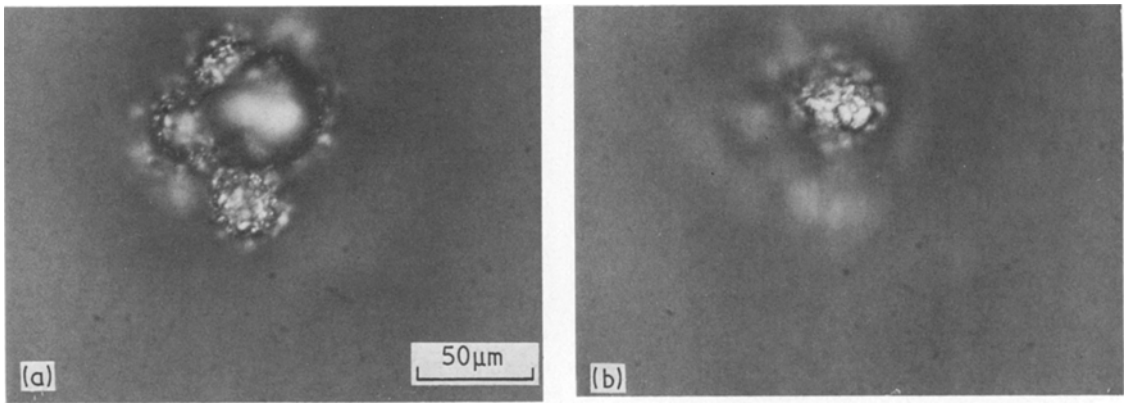

Fig. 4. The effect of hydrogen formation on cathode deposition (CVD = 2.25 V; i_c = 140 mA cm^{-2}; B_z = 374 mT; T = 60° C; C = 0.6 mol dm^{-3}; t_e = 14 min; s = 8 mm). (a) Hydrogen evolution and (b) copper deposition.

electrode is determined by electric–magnetic field interactions, hence twinned and secondary orientations [12] may be expected (90° alignment from the principal direction is most common). This orientation phenomenon may be the cause of the screen-type deposition shown in Fig. 2, where the main orientation is parallel to the imposed magnetic field lines. The pattern seen in Figs. 1, 3, 4 and 5 might be due to large crystal formations due to surface-diffusion-induced coalescence of small crystals; this process has been discussed by Alpress and Sanders [12]. The phenomena described above are also influenced by the presence of gases produced electrolytically; the absence of hydrogen chemisorption on copper [13] and the relative slowness of chemisorption of anodic oxygen on a cathodic copper film [14] may account partially for the tunnel-shape deposits; the inclination angle of about 30° shown in Fig. 5b is in good agreement with the inclination angle range of 14.5–30° reported earlier [15].

The effect of temperature on deposit morphology is more difficult to trace in spite of some recent findings concerning the formation of thin chromium films [16], where micrograins have been observed to form arrays 0.5–0.7 nm apart. These micrograins probably affect the local epitaxial growth of the film and under certain circumstances disordered array patterns may result. By varying the substrate temperature,

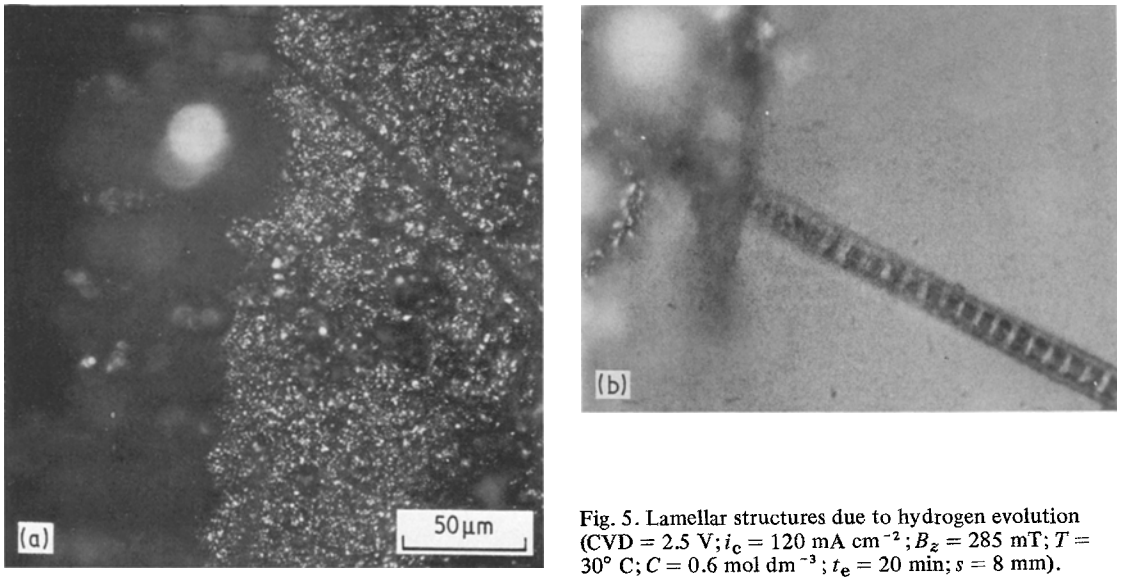

Fig. 5. Lamellar structures due to hydrogen evolution (CVD = 2.5 V; i_c = 120 mA cm^{-2}; B_z = 285 mT; T = 30° C; C = 0.6 mol dm^{-3}; t_e = 20 min; s = 8 mm).

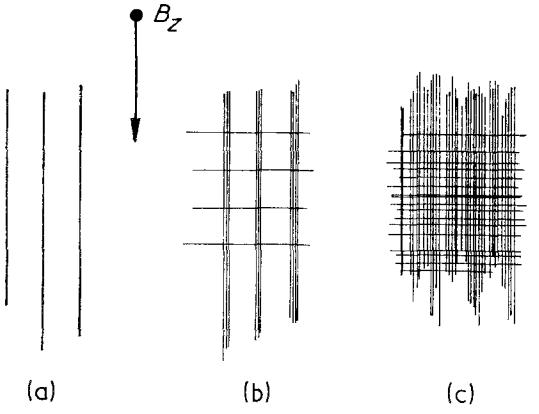

Fig. 6. The development of a screen-type copper deposit on a stainless steel cathode. (a) Initial deposit aligned parallel to the magnetic field lines, (b) the appearance of cross-deposits during continued deposition in the vertical direction, (c) eventual appearance of the closely woven deposition structure.

changes in the film structure can be brought about and transition from crystalline to amorphous deposition may occur. Nevertheless, when a magnetic field is imposed, the combined effect shows predominance of the magnetic field contribution (e.g. [3]) in the sense that bright coherent deposits can easily be obtained within a practical temperature range (15–50° C).

In summary, the screen-type formation of copper deposits on a 316 stainless steel surface during electrolysis may be ascribed primarily to magnetic field imposition and its development is most likely the one illustrated in Fig. 6. Tunnel-shape structures at 30–45° inclination angles are caused by hydrogen evolution at the same time as copper deposition, as shown in Fig. 5. Temperature effects are relatively minor in the presence of the magnetic field and hydrogen evolution.

There remain, of course, a number of aspects of magnetoelectrolytic copper deposition on a stainless steel surface which require further studies for a clear understanding of the overall process. One intriguing question is the possible influence of the

$$Cu^{2+} \xrightarrow{k_1} Cu^{+} \xrightarrow{k_2} Cu$$

kinetics on deposit morphology ($k_1 = 1.86 \times 10^{-4}$ s^{-1} at 55° C and is apparently independent of the Cu^{2+} ion concentration; the associated diffusion-layer barrier = 0.6 mm [17]) as a function of the imposed magnetic field strength. Pulse plating [18] combined with magnetically assisted electrolysis may throw further light on deposition mechanisms.

Acknowledgement

This project has been supported by a Natural Sciences and Engineering Research Council of Canada grant.

References

[1] M. I. Ismail and T. Z. Fahidy, *Can. J. Chem. Eng.* 57 (1979) 734.
[2] *Idem, ibid* 58 (1980) 505.
[3] S. Mohanta and T. Z. Fahidy, *ibid* 50 (1972) 248.
[4] C. W. M. P. Sillen, *Comm. Eur. Commun. Rep. EUR 6085: Seminar on Hydrogen Energy Vector, Production, Use and Transport 337* (1978).
[5] E. J. Kelly, *J. Electrochem. Soc.* 124 (1977) 987.
[6] L. N. Sviridova and V. N. Korshunov, *Electrokhim.* 14 (1978) 99.
[7] E. Z. Gak, E. E. Rokhinson and N. F. Bondarenko, *Elect. Obrab. Mater.* 4 (1976) 62.
[8] V. N. Duradzhi and I. V. Briantzev, *ibid* 5 (1979) 15.
[9] V. B. Evdokimov, A. P. Kravtchinski and B. G. Tichomirov, *Z. Fiz. Khim.* 52 (1978) 644.
[10] F. Ogburn, B. Paretzkin and H. S. Peisser, *Acta Crystallogr.* 17 (1964) 774.
[11] J. G. Alpress and J. V. Sanders, *Aust. J. Phys.* 23 (1970) 23.
[12] *Idem, Surf. Sci.* 7 (1967) 1.
[13] G. L. J. Bailey and H. C. Watkins, *Proc. Phys. Soc. London* B63 (1950) 350.
[14] N. J. Taylor, *Surf. Sci.* 4 (1966) 161.
[15] Vu Thiem Binh, Y. Moulin, R. Uzau and M. Drechsler, *ibid* 79 (1979) 133.
[16] T. Imura, *Japan J. Appl. Phys.* 19 (1980) 215.
[17] G. V. Makarov, *Z. Fiz. Khim.* 54 (1980) 598.
[18] M. K. Ng, A. C. C. Tseung and D. B. Hilbert, *J. Electrochem. Soc.* 127 (1980) 1034.